How to cite: *Angew. Chem. Int. Ed.* **2025**, e20146
doi.org/10.1002/anie.202520146

Ion Channels **Hot Paper**

Flexible Crown-Ether Polyimides Break the K^+/Na^+ Selectivity Barrier in Artificial K^+ Channels

Fei Gou, Yilin Yao, Qiuting Wang, Qingyan Liu, Fuzhen Zheng, Wenju Chang, Jie Shen, and Huaqiang Zeng**

Abstract: Natural potassium channels such as KcsA exhibit extraordinary K^+/Na^+ selectivity (>1000), whereas the best biomimetic counterparts have reached only 41.3. To close this performance gap, we developed a modular design comprising three tunable components: a flexible aliphatic polyimide (**PI**) backbone, variable alkyl linkers (C_nH_{2n+1}, n = 4–16), and ion-binding 18-crown-6 units. This architecture promotes robust membrane integration via the **PI** scaffold and precise control of crown ether conformation and spatial arrangement through linker optimization, enabling exceptionally selective and efficient K^+ transport. Of four synthesized polymer channels, three display high K^+ conductance (36.8–47.0 pS) —up to twice that of gramicidin A (23.2 pS) —together with K^+/Na^+ selectivity exceeding 100. Notably, channel **4**, incorporating the longest $C_{16}H_{33}$ linker, achieves an unprecedented selectivity of 153.2 ± 5.3. This synergistic combination of ultrahigh selectivity and superior conductance establishes a new benchmark for artificial potassium channels and provides a versatile platform for biomimetic membrane technologies, channel-targeted therapeutics, and biosensing applications.

Ion channel proteins are essential molecular machines that sustain life by enabling highly efficient and selective transmembrane ion transport. They maintain electrochemical gradients, mediate signal transduction, and govern processes such as cardiac rhythm and muscle contraction.[1–3] Malfunction can cause severe disorders, including arrhythmias, epilepsy, neonatal diabetes, and cystic fibrosis.[4,5] Natural ion channels display remarkable selectivity and throughput: aquaporin 1 transports 1.1 × 10^{10} water molecules per second while excluding salts and protons,[6,7] KcsA potassium channels achieve K^+/Na^+ selectivity of 10^3,[8] ENaC sodium channels exhibit Na^+/K^+ selectivity > 500,[9,10] and M2 proton channels show 10^5-fold preference for protons over other monovalent cations.[11] Yet translating this extraordinary performance into practical technologies—including drug discovery, membrane separations, and biosensing—remains challenging, hindered by complex self-assembly requirements and acute sensitivity to factors such as temperature, pH, and ionic strength.[12,13]

Inspired by nature's design principles, researchers are advancing artificial ion channels with transport properties approaching those of biological systems, marking a new frontier in supramolecular chemistry.[14–22] In recent years, progress has accelerated markedly. While artificial water channels now surpass natural aquaporins by 150% in water permeability with complete rejection of salt and proton,[23] synthetic proton channels exhibit exceptional selectivity—167.6-fold over Cl^-, 122.7-fold over Na^+, and 81.5-fold over K^+—with proton transport rates 1.22 times higher than those of gramicidin A.[24] Moreover, with Li^+/Na^+ and Li^+/K^+ selectivity ratios reaching 10–20 fold, artificial lithium channels[25–27] attain a level of discrimination with no counterpart in biology.

Yet, even with these advances, instances where artificial channels rival or exceed natural protein performance remain rare. In particular, for biologically relevant K^+,[28–38] Na^+,[39,40] and Cl^- ions,[14,41–48] synthetic systems still fall well short of biological benchmarks. Over the past decade, single-molecule and supramolecular strategies have yielded artificial potassium channels with ultrafast K^+ conduction and steadily improving K^+/Na^+ selectivity—from 9.8 in 2017[33] to 20.1 in 2023,[36,37] and most recently 41.3 in 2025.[38] Yet these values remain far below the ~1000:1 selectivity of KcsA channels, highlighting the formidable challenges that persist.

Polymers offer distinct advantages for constructing transmembrane channels across the ~3 nm hydrophobic core of cell membranes, owing to their facile synthesis and structural versatility.[23,26,27,31,35,49] Polyimides are particularly attractive because of their exceptional chemical, thermal, and

[*] Dr. F. Gou, Ms. Y. Yao, Ms. Q. Wang, Dr. W. Chang, Prof. Dr. J. Shen, Prof. Dr. H. Zeng
College of Chemistry, Fuzhou University, Fuzhou, Fujian 350116, China
E-mail: shenJie@fzu.edu.cn
hqzeng@fzu.edu.cn

Ms. Q. Liu
State Key Laboratory of Structural Chemistry, and Fujian Key, Laboratory of Nanomaterials, Fujian Institute of Research on the Structure of Matter Chinese Academy of Sciences, Fuzhou, Fujian 350002, China

Dr. F. Zheng
Department of Cardiovascular Surgery, Fuzhou University Affiliated Provincial Hospital, Fuzhou, Fujian 350116, China

Artificial K^+ channels https://doi.org/10.1002/anie.200(will be filled in by the editorial staff)

Additional supporting information can be found online in the Supporting Information section

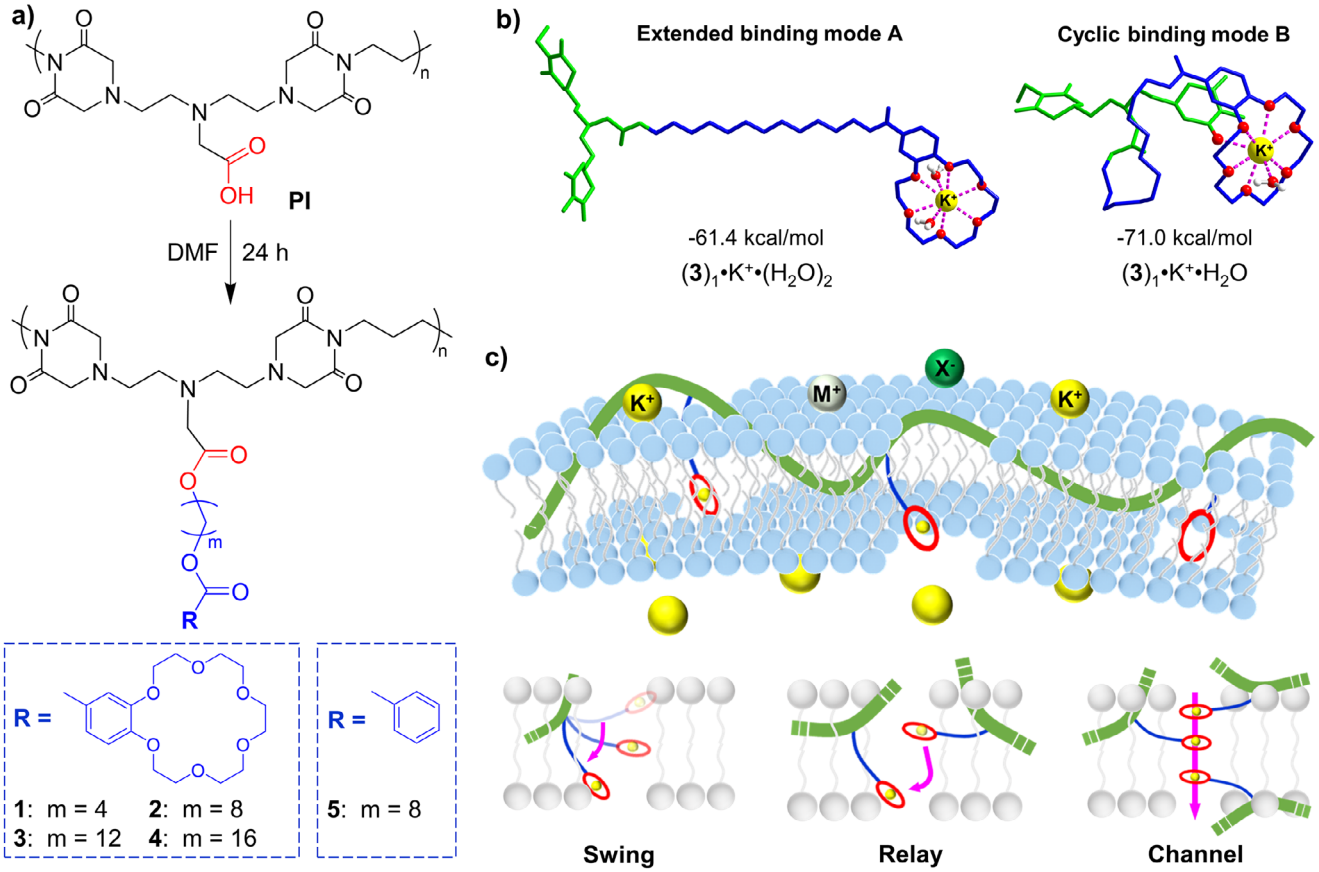

Figure 1. Molecular design and schematic of a polyimide-based 18-crown-6-modified modular system as K^+-selective channels. a) Synthesis of **PI**-based polymer channels **1**–**4**, bearing benzo-18-crown-6 structural units connected via alkyl chains of varying lengths. b) DFT-optimized structures and binding energies computed at the M06-2X/6–311 + G(d,p)//M06-2X/6–31G(d) level of theory for extended binding mode **A** and cyclic binding mode **B**, involving $(\mathbf{3})_1$, made of one repeating unit from **3**, with a K^+ ion. c) Schematic representation of a channel molecule embedded in a bilayer membrane, illustrating three possible ion transport mechanisms: molecular swing, molecular relay, and self-assembled channel. Notably, the crown ether units participating in ion transport via the relay and channel mechanisms may derive from either a single polymer molecule or multiple polymer molecules.

mechanical stability, as well as their ease of functionalization and film formation.[50,51] However, conventional aromatic **PI**s show poor compatibility with phospholipid bilayers, largely due to the mismatch between their rigid backbones and the flexible lipid tails. Likewise, although 18-crown-6 ethers are widely used in artificial channels for their strong K^+ binding, this affinity often does not translate into high selectivity or efficient transmembrane transport, reflecting incomplete understanding of the "capture–release" equilibrium at membrane interfaces and within bilayers.

To overcome these challenges and address the long-standing selectivity bottleneck in artificial K^+ channels, we developed a hybrid system integrating a polyimide scaffold with 18-crown-6 units (Figure 1a). This design strategy features three key elements: (1) engineering a flexible **PI** backbone from morpholine-2,6-dione and diaminopropane to enhance membrane integration and stability; (2) covalently tethering 18- crown-6, serving as ion capture and transport units, to carboxyl-functionalized **PI** through tunable alkyl linkers, thereby endowing the otherwise inactive polymer with K^+ transport capability; and (3) systematically varying the linker length (C_nH_{2n+1}, $n = 4$–16) to control the conformation and spatial orientation of 18-crown-6, thereby modulating both ion binding (Figure 1b) and transport (Figure 1c) property.

This **PI**-supported modular strategy has produced the first polyimide-based artificial potassium channels that combine high K^+ transport efficiency with exceptional K^+/Na^+ selectivity. Single channel current recordings reveal robust K^+ conductance (36.8–47.0 pS) and selectivity exceeding 100. Most notably, the $C_{16}H_{33}$-modified channel **4** achieves an unprecedented K^+/Na^+ selectivity factor of 153.2 ± 5.3, establishing a new benchmark for artificial potassium channels and representing a major step toward fully biomimetic membrane systems.

Building upon the demonstrated potential of polymer scaffolds in transmembrane transport,[23,26–27,31,35,49] this study introduces novel aliphatic polyimide-based architectures aimed at overcoming critical performance limitations of artificial ion channels. While aromatic polyimides provide exceptional structural robustness, their pronounced hydrophobicity reduces compatibility with phospholipid membranes, leading to precipitation. To improve the ability of polymer molecules to insert into membranes, we synthesized a

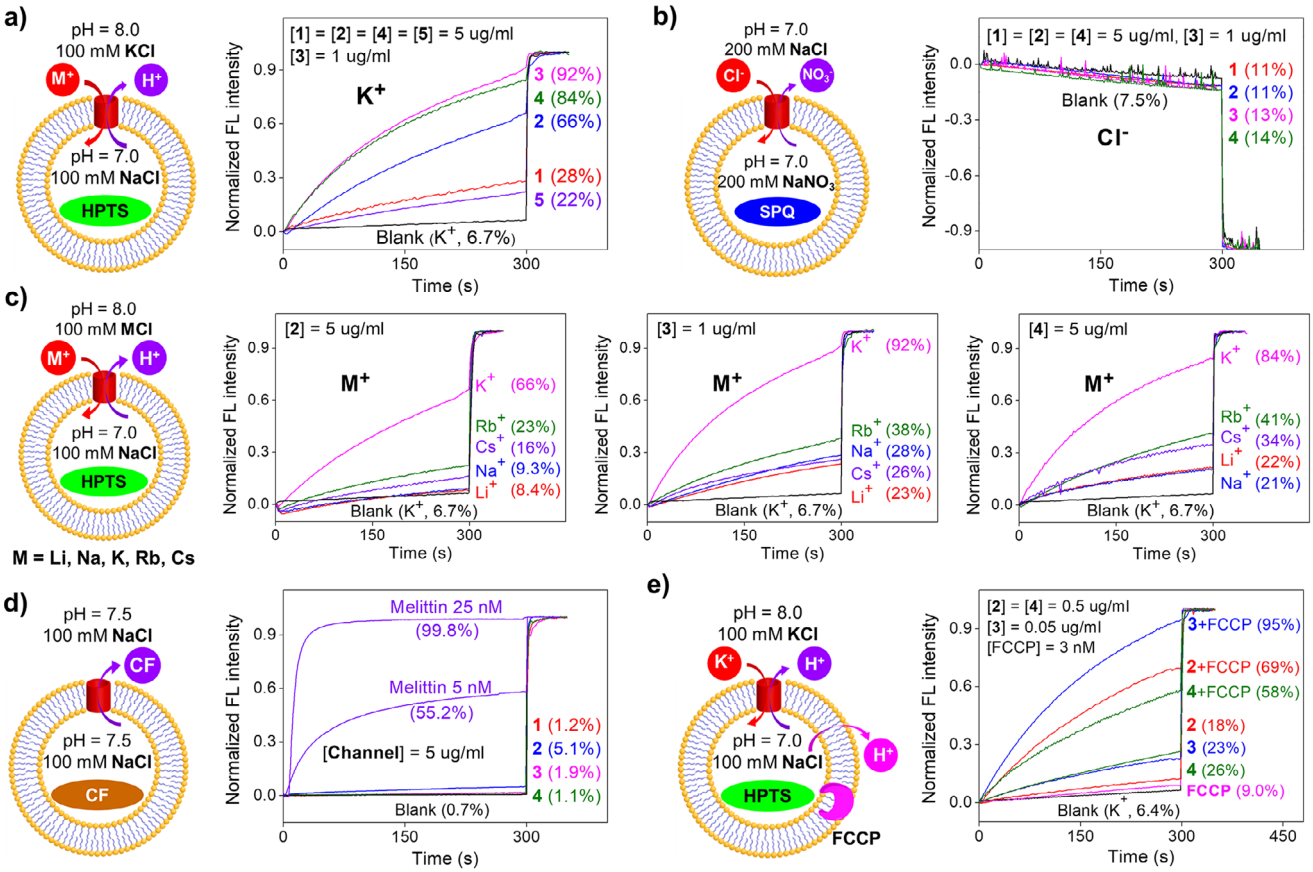

Figure 2. a) and c) The DOPC-based pH-sensitive HPTS assay for comparing ion transport activities and selectivities of **1**–**5**, with extravesicular salts being MCl (M = Li, Na, K, Rb, and Cs). b) The chloride-sensitive SPQ assay for assessing the chloride transport activities of **1**–**4**. d) CF dye leakage assay to confirm the membrane integrity in the presence of **1**–**4**. e) The HPTS assay in the presence of proton carrier FCCP to compare the relative ion transport rate between H^+ and K^+. DOPC = dioleoyl phosphatidylcholine, HPTS = 8-hydroxypyrene-1,3,6-trisulfonic acid trisodium salt, SPQ = (6-methoxy-N-(3-sulfopropyl))quinolinium, CF = 5(6)-carboxy fluorescein and FCCP = carbonyl cyanide 4-(trifluoromethoxy) phenylhydrazone.

flexible, heteroatom-rich, carboxyl-containing **PI** backbone (Figure 1a) via a one-pot reaction between diethylenetriaminepentaacetic dianhydride and diaminopropane at 180 °C (Scheme S1). Gel permeation chromatography (GPC) analysis gives an average molecular weight of ~14,000 Da with ~35 carboxylic acid groups for **PI** (Table S2), providing versatile sites for subsequent functionalization.

We next covalently grafted crown ether moieties onto the **PI** backbone using ester linkages with systematically tuned alkyl spacers (C_nH_{2n+1}, n = 4, 8, 12, and 16; Figure 1a and Scheme S1). Successful grafting is evident from marked differences in solubility: whereas the **PI** polymer dissolves readily (>50 mg/mL) in $CHCl_3$, DMF, and DMSO, polymers **1**–**4** are nearly insoluble in $CHCl_3$ and DMF and exhibit moderate solubility (>20 mg/mL) in DMSO (Table S1). Polymer NMR characterization also confirms that crown ether groups have been modified onto the **PI** polymer (Figures S22–S26). Such covalent attachment harnesses alkyl-chain flexibility to precisely control crown ether orientation in lipid bilayers, swing amplitude during ion transfer, and spatial distribution along the polymer backbone. Based on the GPC-derived molecular weights of 18018, 21639, 22541, and 21,437 Da, respectively, these functionalizations afford polymers **1**–**4**, in which approximately 22%, 29%, 38%, and 34% of the carboxylate sites were modified with crown ethers (Table S2). Furthermore, given the strong correlation between the polymer's C/O mass ratio (M_C/M_O) and the degree of crown ether functionalization (Table S3) and that some difficult-to-remove Cs^+ ions present in all polymer samples (Figure S1) compromised the accuracy of elemental analysis, EDS analysis was employed to determine the extent of functionalization in polymers **1**–**4** (Figure S2). Compared to the unmodified **PI** polymer (M_C/M_O = 2.12), the M_C/M_O values of polymers **1**–**4** gradually increased (Table S4). The functionalization ratio, calculated from the EDS data, was approximately 30%, 30%, and 40% for polymers **2**–**4**. The result for polymer **1** was less reliable due to its much smaller change in M_C/M_O before and after functionalization Overall, the functionalization ratios derived from EDS for polymers **2**–**4** show great consistency with the GPC data. For comparison, a crown ether–free polymer (**5**) was also synthesized (Figure 1a and Scheme S2).

We hypothesize that the flexible polymer backbone facilitates adaptive intercalation into phospholipid membranes,

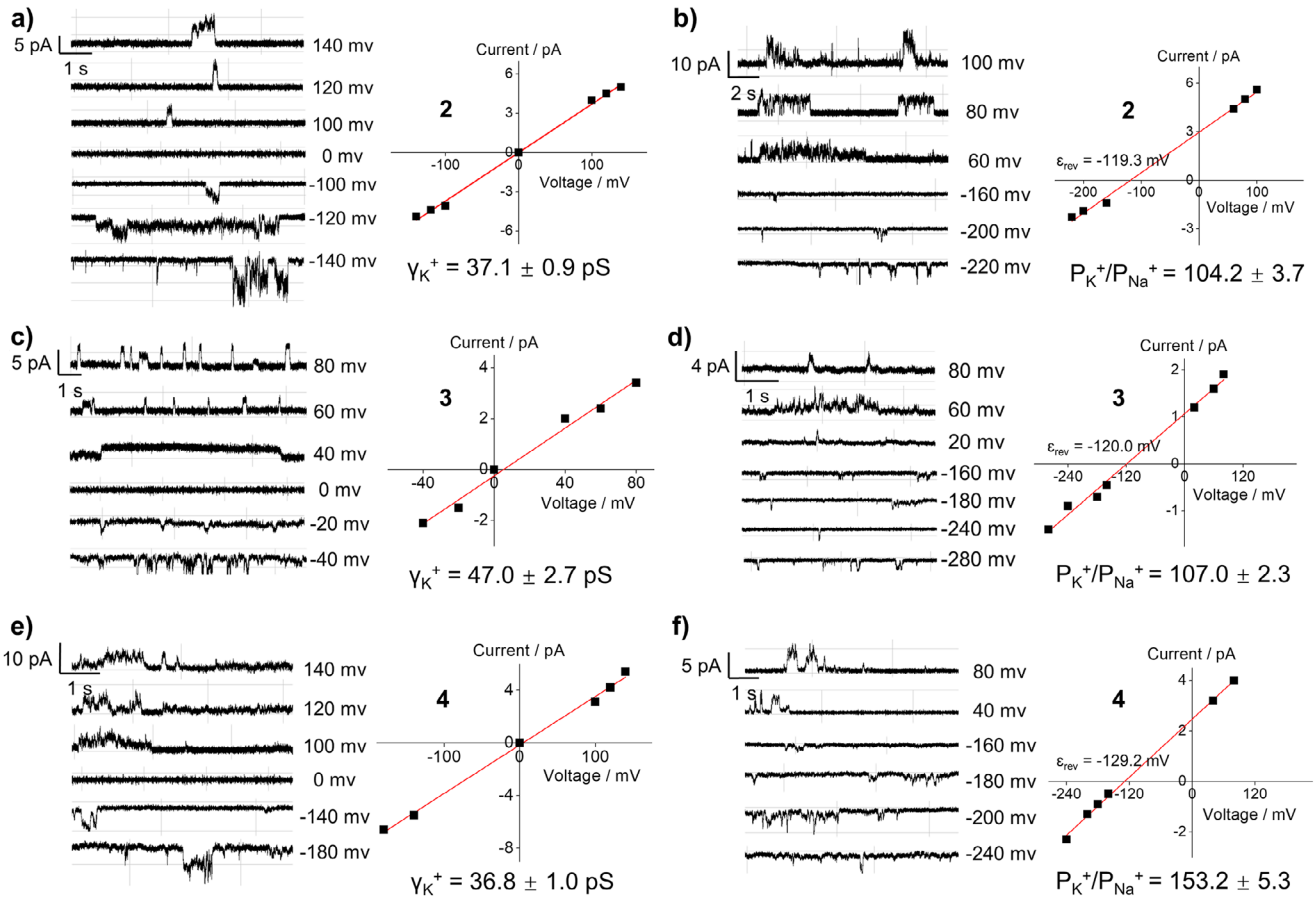

Figure 3. Single channel current traces and current–voltage (I-V) curves recorded for **2**–**4**. a), c), and e) With *cis* chamber = *trans* chamber = 1 M KCl, the potassium conduction rate (γ_{K^+}) values were determined to be 37.0 ± 0.9 pS for **2** a), 47.0 ± 2.7 pS for **3** c), and 36.8 ± 1.0 pS for **4** e), respectively. b), d), and f) With *cis* chamber = 1 M KCl and *trans* chamber = 1 M NaCl, the P_{K^+}/P_{Na^+} selectivity factors were determined to be 104.2 ± 3.7 for **2** (b), 107 ± 2.3 for **3** (d), and 153.2 ± 5.3 for **4** (f), respectively. Here, γ_{K^+} values were obtained by fitting the I-V curves using a linear equation of $y = a + b*x$ where slope b is γ in the unit of nS. P_{K^+}/P_{Na^+} values were calculated using a simplified Goldman-Hodgkin-Katz equation $\varepsilon_{rev} = RT/F \times \ln(P_{Na^+}/P_{K^+})$, where R = universal gas constant (8.314 J·K^{-1} mol^{-1}), T = 298 K, F = Faraday's constant (96485 C·mol^{-1}), and P is the ion permeability. All single channel current traces were recorded in a diPhyPC-based bilayer membrane.
diPhyPC = 1,2-diphytanoyl-sn-glycero-3-phosphocholine.

with crown ether termini spontaneously embedding within the hydrophobic core. Based on relevant research reports,[52–62] we further propose three non-exclusive mechanisms for promoting efficient and selective transmembrane K^+ transport (Figure 1c): (1) Swing mechanism – K^+ binding at the membrane interface triggers an alkyl chain–mediated pendulum-like motion, facilitating ion translocation;[52–56] (2) Relay mechanism – following K^+ binding, crown ether moieties swing toward the hydrophobic core, where proximity-driven relay conduction between adjacent sites on the polymer backbone enables transmembrane ion transfer;[57–60] and (3) Channel mechanism – crown ether units from one single or multiple polymer chains converge to self-assemble into K^+-conductive channels within the hydrophobic layer.[30,35–38,61–62] Given the complexity of ion transport by these polymer-based transporters, we believe that the polymer does not operate via a single mechanism but leverages a dynamic integration of different processes, forming a cooperative network to achieve high-efficiency ion transmembrane transport.

The UV-Vis spectroscopy measurements in acetonitrile reveal that polymers **1**–**4** exhibit significantly enhanced UV absorption accompanied by observable precipitation upon the addition of KCl, whereas they show negligible responses to other alkali metal salts (Figure S3). These results confirm their selective recognition capability toward K^+ ions. Meanwhile, in the LUV test system, we used UV-Vis spectroscopy to monitor the interaction between blank liposomes (without loaded HPTS) and polymer in the presence of alkali metal ions. The results showed that after the addition of K^+, the UV absorption spectrum of polymer **3** underwent significant changes compared to when Li^+ or Na^+ was added, but no precipitate formation was induced (Figure S4). This phenomenon further confirms the selective recognition ability of this series of polymers for K^+ and suggests their potential transport function. Binding energy calculations were performed on two possible binding modes **A** and **B** for **2**–**4**, each containing one repeating unit, one K^+ ion and up to two H_2O molecules (Figures 1b and S5). Calculations show that the extended binding mode **A** is less stable than the cyclic binding mode

B by 9.9 kcal/mol for **2** (Figure S5a), 9.6 kcal/mol for **3** (Figure 1b) and 5.3 kcal/mol for **4** (Figure S5b). These comparative data suggest that the polymers preferentially adopt the thermodynamically favored mode **B** conformation for K^+ binding and transport. Furthermore, the energy gap between mode **A** and mode **B** decreases from approximately 10 kcal/mol for both **2** and **3** to 5.3 kcal/mol for **4**, underscoring the critical role of alkyl spacer length in modulating K^+ capture and transport property.

Prompted by the spectroscopic titration and computational findings, we quantified ion transport activities of crown ether-functionalized **1**–**4** and the phenyl-modified control **5** using a vesicle-based HPTS assay. This method employs pH-sensitive HPTS dye encapsulated within DOPC-based large unilamellar vesicles (LUVs), an imposed proton gradient (from pH 7.0 to 8.0) and extravesicular 100 mM KCl (Figure 2a). Using this method, **1** and **5** show minimal K^+ transport (28% and 22% at 5 μg/mL, Figure S7), whereas **2** and **4** reach 66% and 84%, and **3** exhibits outstanding activity—achieving 92% efficiency at only 1 μg/mL (Figure 2a). Furthermore, the high potassium ion transport activity of Polymer 3 is underscored by the reproducible K^+/Na^+ transport activity and selectivity observed in LUV assays across three independent batches (Figure S8).

The anion transport activity of **1**–**4** was assessed using the SPQ fluorescence quenching assay, which utilizes a Cl^--sensitive fluorophore whose emission is selectively quenched by Cl^- ions. As illustrated in Figure 2b, 1–4 induce no significant change in SPQ fluorescence intensity upon addition, confirming their inability to transport Cl^- ions.

Using the same HPTS assay with extravesicular salts MCl (M = Li, Na, K, Rb, and Cs; Figure 2c), 2–4 exhibit remarkable potassium selectivity, with $EC_{50}(K^+)$ values of 3.3, 0.22, and 1.9 μg/mL, respectively (Figure S9). Polymer **3** demonstrated the best K^+ transport performance—nearly tenfold greater than that of **2** and **4**.

Membrane integrity was evaluated using CF dye leakage assays (Figures 2d and S10). At 5 μg/mL, **1**–**4** induce only 1.1%–5.1% leakage, values that are far below the pore-forming control melittin, causing 55%and 100% leakage at 5 and 25 nM, respectively. These findings confirm the structural integrity of LUV membranes in the presence of **1**–**4** and therefore rule out membrane disruption or formation of large pores as mechanisms of ion transport by **1**–**4**.

To compare the relative rate between K^+ and H^+, HPTS assays were conducted in the presence of a protonophore FCCP (Figure 2e). FCCP accelerates delayed H^+ counter-transport during K^+ influx, producing fluorescence enhancement. The transport efficiencies are 9% for FCCP alone, and 18%, 23%, and 26% for compounds **2**, **3**, and **4** alone, respectively. In the presence of FCCP, compounds **2**, **3**, and **4** exhibit markedly enhanced efficiencies of 48% (69% – 18% – (9.0%–6.4%)), 69% (95% – 23% – (9.0%–6.4%)), and 29% (58% – 26% – (9.0%–6.4%)), respectively. These significant enhancements confirm that K^+ flux is the dominant process.

Single-channel electrophysiological studies using a planar lipid bilayer workstation were performed to quantify ion transport selectivity and elucidate mechanistic behavior of channels **2**–**4**.

Under symmetric ionic conditions (1 M KCl in both *cis* and *trans* chambers; Figure S11), **2**–**4** exhibit characteristic square-wave currents, unambiguously confirming a well-defined channel-type transport mechanism (Figure 3a,c, and e). Unitary K^+ conductance values (γ_{K^+}) were measured as 37.1 ± 0.9 pS (**2**), 47.0 ± 2.7 pS (**3**), and 36.8 ± 1.0 pS (**4**), transporting K^+ ions at ultrafast rates 160–200% faster than gramicidin A ($\gamma_{K^+} = 23.2 \pm 0.4$ pS).[33]

K^+/Na^+ transport selectivity was probed under asymmetric conditions (*cis* chamber = 1 M KCl and *trans* chamber = 1 M NaCl). Analysis of current-voltage (I-V) curves (Figure 3b,d, and f) yield reversal potentials (ε_{rev}) of 119.3 mV (**2**), 120.0 mV (**3**), and 129.2 mV (**4**), corresponding to K^+/Na^+ permeability ratios of 104.2 ± 3.7, 107.0 ± 2.3, and 153.2 ± 5.3, respectively. Although precisely deconvoluting the origin of such high selectivity remains challenging, two structural factors appear decisive: the linker length and the degree of crown ether functionalization. Both contribute to modulating the dynamic process of ion capture and release. Nevertheless, the system's unprecedented selectivity ($K^+/Na^+ > 150$ for **4**), coupled with its ultrafast K^+ conduction, successfully overcomes the classical trade-off between conduction speed and ion discrimination in artificial ion channels.

In conclusion, this study overcomes the critical limitation of low K^+/Na^+ selectivity (~40) in artificial potassium channels—compared with natural KcsA channels (~1000) — through an innovative modular strategy comprising a flexible polyimide backbone, tunable alkyl spacers, and 18-crown-6 ether ionophores. The approach delivers advances in three areas: a) a flexible **PI** backbone mitigates the membrane incompatibility of rigid scaffolds; b) covalent anchoring of 18-crown-6 via systematically varied alkyl spacers allows precise control over crown-ether conformation, orientation, and ion-binding/release kinetics; and c) bilayer lipid membrane measurements reveal exceptional K^+ conductance (36.8–47.0 pS) across channels **2**–**4**, with **4** achieving a record-high K^+/Na^+ selectivity of 153.2 ± 5.3. This modular "flexible backbone–tunable spacer–functional unit" design establishes a versatile platform for high-performance artificial ion channels, with transformative potential in biomimetic membrane separations, channelopathy-targeted therapeutics, and precision biosensing.

Acknowledgements

The authors greatly appreciate the support of this work by the National Natural Science Foundation of China (22271049 and 22371048), the "Chu ying Program" for the Top Young Talents of Fujian Province, the Postdoctoral Fellowship Program of CPSF under Grant Number GZC20230455, the Natural Science Foundation of Fujian Province (2023J01054) and a start-up grant from Fuzhou University.

Conflict of Interests

The authors declare no conflict of interest.

Data Availability Statement

The data that support the findings of this study are available from the corresponding author upon reasonable request.

Keywords: Artificial potassium channels · Crown ether · Polyimide · Supramolecular chemistry · Transmembrane transport

[1] T. J. Jentsch, C. A. Hübner, J. C. Fuhrmann, *Nat. Cell Biol.* **2004**, *6*, 1039–1047, https://doi.org/10.1038/ncb1104-1039.

[2] L.-O. Essen, U. Koert, *Annu. Rep. Prog. Chem. Sect. C: Phys. Chem.* **2008**, *104*, 165, https://doi.org/10.1039/b703980h.

[3] J. W. F. Robertson, J. J. Kasianowicz, S. Banerjee, *Chem. Rev.* **2012**, *112*, 6227–6249, https://doi.org/10.1021/cr300317z.

[4] M. A. Zaydman, J. R. Silva, J. Cui, *Chem. Rev.* **2012**, *112*, 6319–6333, https://doi.org/10.1021/cr300360k.

[5] S. Bajaj, S. T. Ong, K. G. Chandy, *Nat. Prod. Rep.* **2020**, *37*, 703–716, https://doi.org/10.1039/C9NP00056A.

[6] K. Murata, K. Mitsuoka, T. Hirai, T. Walz, P. Agre, J. B. Heymann, A. Engel, Y. Fujiyoshi, *Nature* **2000**, *407*, 599–605, https://doi.org/10.1038/35036519.

[7] A. Horner, F. Zocher, J. Preiner, N. Ollinger, C. Siligan, S. A. Akimov, P. Pohl, *Sci. Adv.* **2015**, *1*, e1400083.

[8] T. Dudev, C. Lim, *J. Am. Chem. Soc.* **2009**, *131*, 8092–8101.

[9] L. G. Palmer, *J. Membr. Biol.* **1982**, *67*, 91–98, https://doi.org/10.1007/BF01868651.

[10] T. Dudev, C. Lim, *J. Am. Chem. Soc.* **2010**, *132*, 2321–2332, https://doi.org/10.1021/ja909280g.

[11] J. A. Mould, H.-C. Li, C. S. Dudlak, J. D. Lear, A. Pekosz, R. A. Lamb, L. H. Pinto, *J. Biol. Chem.* **2000**, *275*, 8592–8599, https://doi.org/10.1074/jbc.275.12.8592.

[12] H. Ryu, A. Fuwad, S. Yoon, H. Jang, J. C. Lee, S, M., Kim, T.-J. J., *Int. J. Mol. Sci.* **2019**, *20*, 1437, https://doi.org/10.3390/ijms20061437.

[13] C. M. Nimigean, *Nature* **2022**, *608*, 670–672, https://doi.org/10.1038/d41586-022-02163-3.

[14] X. Wu, A. M. Gilchrist, P. A. Gale, *Chem* **2020**, *6*, 1296–1309, https://doi.org/10.1016/j.chempr.2020.05.001.

[15] S.-P. Zheng, L.-B. Huang, Z. Sun, M. Barboiu, *Angew. Chem. Int. Ed.* **2021**, *60*, 566–597, https://doi.org/10.1002/anie.201915287.

[16] K. Sato, T. Muraoka,K. Kinbara, *Acc. Chem. Res.* **2021**, *54*, 3700–3709, https://doi.org/10.1021/acs.accounts.1c00397.

[17] J. Shen, C. Ren, H. Q. Zeng, *Acc. Chem. Res.* **2022**, *55*, 1148–1159, https://doi.org/10.1021/acs.accounts.1c00804.

[18] A. Mondal, M. Ahmad, D. Mondal, P. Talukdar, *Chem. Commun.* **2023**, *59*, 1917–1938, https://doi.org/10.1039/D2CC06761G.

[19] M. Ahmad, S. A. Gartland, M. J. Langton, *Angew. Chem. Int. Ed.* **2023**, *62*, e202308842.

[20] X. Yuan, J. Shen, H. Q. Zeng, *Chem. Commun.* **2024**, *60*, 482–500, https://doi.org/10.1039/D3CC04488B.

[21] D. Zhang, W. Chang, J. Shen, H. Q. Zeng, *Chem. Commun.* **2024**, *60*, 13468–13491, https://doi.org/10.1039/D4CC04388J.

[22] T. Yan, J. Liu, *Angew. Chem. In. Ed.* **2025**, *64*, e202416200.

[23] A. Roy, J. Shen, H. Joshi, W. Song, Y.-M. Tu, R. Chowdhury, R. Ye, N. Li, C. Ren, M. Kumar, A. Aksimentiev, H. Q. Zeng, *Nat. Nanotech.* **2021**, *16*, 911–917, https://doi.org/10.1038/s41565-021-00915-2.

[24] J. Shen, R. Ye, Z. Liu, H. Q. Zeng, *Angew. Chem. Int. Ed.* **2022**, *61*, e202200259, https://doi.org/10.1002/anie.202200259.

[25] L. Zhang, C. Zhang, X. Dong, Z. Dong, *Angew. Chem. Int. Ed.* **2023**, *62*, e202214194.

[26] J. Shen, Z, Y. L.i, H. Oh, H. Behera, H. Joshi, M. Kumar, A. Aksimentiev, H. Q. Zeng, *Angew. Chem. Int. Ed.* **2023**, *62*, e202305623.

[27] F. Gou, Q. Wang, Z. Yang, W. Chang, J. Shen, H. Q. Zeng, *Angew. Chem. Int. Ed.* **2025**, *64*, e202418304, https://doi.org/10.1002/anie.202418304.

[28] A. Gilles, M. Barboiu, *J. Am. Chem. Soc.* **2016**, *138*, 426–432, https://doi.org/10.1021/jacs.5b11743.

[29] C. Lang, X. Deng, F. Yang, B. Yang, W. Wang, S. Qi, X. Zhang, C. Zhang, Z. Dong, J. Liu, *Angew. Chem. Int. Ed.* **2017**, *56*, 12668–12671, https://doi.org/10.1002/anie.201705048.

[30] C. Ren, J. Shen, H. Q. Zeng, *J. Am. Chem. Soc.* **2017**, *139*, 12338–12341, https://doi.org/10.1021/jacs.7b04335.

[31] F. Chen, J. Shen, N. Li, A. Roy, R. Ye, C. Ren, H. Q. Zeng, *Angew. Chem. Int. Ed.* **2020**, *59*, 1440–1444, https://doi.org/10.1002/anie.201906341.

[32] L. Z. Zeng, H. Zhang, T. Wang, T. Li, *Chem. Commun.* **2020**, *56*, 1211–1214, https://doi.org/10.1039/C9CC08396K.

[33] S. Qi, C. Zhang, H. Yu, J. Zhang, T. Yan, Z. Lin, B. Yang, Z. Dong, *J. Am. Chem. Soc.* **2021**, *143*, 3284–3288, https://doi.org/10.1021/jacs.0c12128.

[34] D. Qiao, H. Joshi, H. Zhu, F. Wang, Y. Xu, J. Gao, F. Huang, A. Aksimentiev, J. Feng, *J. Am. Chem. Soc.* **2021**, *143*, 15975–15983, https://doi.org/10.1021/jacs.1c04910.

[35] T. Yan, S. Liu, C. Li, J. Xu, S. Yu, T. Wang, H. Sun, J. Liu, *Angew. Chem. Int. Ed.* **2022**, *61*, e202210214, https://doi.org/10.1002/anie.202210214.

[36] H. Ma, R. Ye, L. Jin, S. Zhou, C. Ren, H. Ren, J. Shen, H. Q. Zeng, *Chin. Chem. Lett.* **2023**, *34*, 108355, https://doi.org/10.1016/j.cclet.2023.108355.

[37] L. Jin, C. Sun, Z. Li, J. Shen, H. Q. Zeng, *Chem. Commun.* **2023**, *59*, 3610–3613, https://doi.org/10.1039/D2CC04396C.

[38] Y. Wu, Q. Xu, Y. Chen, C. Li, Y. Wu, X. Yu, H. Li, Z. Xu, J. Xu, Z. Ni, Y. Ge, T. Yan, Z. Qi, J. Liu, *Adv. Mater.* **2025**, *37*, 2416852, https://doi.org/10.1002/adma.202416852.

[39] F. Otis, C. Racine-Berthiaume, N. Voyer, *J. Am. Chem. Soc.* **2011**, *133*, 6481–6483, https://doi.org/10.1021/ja110336s.

[40] L. Zhang, J. Tian, Z. Lin, Z. Dong, *J. Am. Chem. Soc.* **2024**, *146*, 8500–8507, https://doi.org/10.1021/jacs.3c14736.

[41] V. Gorteau, G. Bollot, J. Mareda, A. Perez-Velasco, S. Matile, *J. Am. Chem. Soc.* **2006**, *128*, 14788–14789, https://doi.org/10.1021/ja0665747.

[42] C. R. Yamnitz, S. Negin, I. A. Carasel, R. K. Winter, G. W. Gokel, *Chem. Commun.* **2010**, *46*, 2838, https://doi.org/10.1039/b924812a.

[43] C. Ren, X. Ding, A. Roy, J. Shen, S. Zhou, F. Chen, S. F. Yau Li, H. Ren, Y. Y. Yang, H. Q. Zeng, *Chem. Sci.* **2018**, *9*, 4044–4051, https://doi.org/10.1039/C8SC00602D.

[44] C. Ren, F. Zeng, J. Shen, F. Chen, A. Roy, S. Zhou, H. Ren, H. Q. Zeng, *J. Am. Chem. Soc.* **2018**, *140*, 8817–8826, https://doi.org/10.1021/jacs.8b04657.

[45] R. Cao, R. B. Rossdeutcher, Y. Zhong, Y. Shen, D. P. Miller, T. A. Sobiech, X. Wu, L. S. Buitrago, K. Ramcharan, M. I. Gutay, M. F. Figueira, P. Luthra, E. Zurek, T. Szyperski, B. Button, Z. Shao, B. Gong, *Nat. Chem.* **2023**, *15*, 1501–1502.

[46] W.-L. Huang, X.-D. Wang, Y.-F. Ao, Q.-Q. Wang, D.-X. Wang, *Angew. Chem. Int. Ed.* **2023**, *62*, e202302198.

[47] R. Sharma, S. Sarkar, S. Chattopadhayay, J. Mondal, P. Talukdar, *Angew. Chem. Int. Ed.* **2024**, *63*, e202319919.

[48] Y. Lin, B. Wu, Y. Zeng, H. Yuan, C. Ji, Z. Liu, Y. Sui, T. Yin, X. Kong, Y. Zhu, J. Chen, C. Lang, *Angew. Chem. Int. Ed.* **2024**, *63*, e202408558, https://doi.org/10.1002/anie.202408558.

[49] T. Jiang, A. Hall, M. Eres, Z. Hemmatian, B. Qiao, Y. Zhou, Z. Ruan, A. D. Couse, W. T. Heller, H. Huang, M. O. de la Cruz, M. Rolandi, T. Xu, *Nature* **2020**, *577*, 216–220, https://doi.org/10.1038/s41586-019-1881-0.

[50] Y. Zhuang, J. G. Seong, Y. M. Lee, *Prog. Polym. Sci.* **2019**, *92*, 35–88, https://doi.org/10.1016/j.progpolymsci.2019.01.004.
[51] M. Zhang, L. Wang, H. Xu, Y. Song, X. He, *Nano-Micro Lett.* **2023**, *15*, 135, https://doi.org/10.1007/s40820-023-01104-7.
[52] R. J. Ye, C. L. Ren, J. Shen, N. Li, F. Chen, A. Roy, H. Q. Zeng, *J. Am. Chem. Soc.* **2019**, *141*, 9788–9792, https://doi.org/10.1021/jacs.9b04096.
[53] C. Ren, F. Chen, R. J. Ye, Y. S. Ong, H. Lu, S. S. Lee, J. Y. Ying, H. Q. Zeng, *Angew. Chem. Int. Ed.* **2019**, *58*, 8034–8038, https://doi.org/10.1002/anie.201901833.
[54] J. Shen, J. J. Y. Han, R. J. Ye, H. Q. Zeng, *Sci. China: Chem.* **2021**, *64*, 2154–2160, https://doi.org/10.1007/s11426-021-1082-7.
[55] S. W. Deng, Z. Y. Li, L. Yuan, H. Q. Zeng, *Nano Lett.* **2024**, *24*, 10750–10758, https://doi.org/10.1021/acs.nanolett.4c01884.
[56] H. Yang, J. Yi, S. Pang, K. Ye, Z. Ye, Q. Duan, Z. Yan, C. Lian, Y. Yang, L. Zhu, D.-H. Qu, C. Bao, *Angew. Chem. Int. Ed.* **2022**, *61*, e202204605, https://doi.org/10.1002/anie.202204605.
[57] B. A. McNally, E. J. O'Neil, A. Nguyen, B. D. Smith, *J. Am. Chem. Soc.* **2008**, *130*, 17274–17275, https://doi.org/10.1021/ja8082363.
[58] T. G. Johnson, A. Sadeghi-Kelishadi, M. J. Langton, *J. Am. Chem. Soc.* **2022**, *144*, 10455–10461., https://doi.org/10.1021/jacs.2c02612.
[59] T. G. Johnson, M. J. Langton, *J. Am. Chem. Soc.* **2023**, *145*, 27167–27184, https://doi.org/10.1021/jacs.3c08877.
[60] Q. Zhang, Q. Liang, G. Wang, X. Xie, Y. Cao, N. Sheng, Z. Zeng, C. Ren, *JACS Au* **2024**, *4*, 3869–3883.
[61] C. Li, Y. Wu, Y. Zhu, J. Yan, S. Liu, J. Xu, S. Fa, T. Yan, D. Zhu,Y. Yan, J. Liu, *Adv. Mater.* **2024**, *36*, 2312352, https://doi.org/10.1002/adma.202312352.
[62] C. Li, Y. Wu, S. Bao, H. Li, Z. Xu, J. Yan, X. Yu, L. He, T. Zhang, W. Liu, S. Hou, Y. Zhang, J. Xu, T. Yan, T. Wang, Y. Yan, J. Liu, *J. Am. Chem. Soc.* **2025**, *147*, 14139–14153, https://doi.org/10.1021/jacs.4c14583.

Manuscript received: September 13, 2025
Revised manuscript received: November 20, 2025
Manuscript accepted: December 01, 2025
Version of record online: ■■, ■■